



Published in final edited form as:

Mol Carcinog. 2015 October ; 54(10): 1122–1131. doi:10.1002/mc.22183.

Enhanced aggressiveness of benzopyrene-induced squamous carcinomas in transgenic mice overexpressing the proprotein convertase PACE4 (PCSK6)

Daniel E. Bassi^{1,2}, Jonathan Cenna¹, Jirong Zhang¹, Edna Cukierman², and Andres J. Klein-Szanto^{1,2}

¹Department of Pathology, Fox Chase Cancer Center, Philadelphia, PA 19111, USA

²Cancer Biology Program, Fox Chase Cancer Center, Philadelphia, PA 19111, USA

Abstract

PACE4 (PCSK6) is a pro-protein convertase (PC) capable of processing numerous substrates involved in tumor growth, invasion, and metastasis. Because of the human relevancy of the tobacco-associated carcinogen benzo[a]pyrene (B(a)P) we investigated whether transgenic mice in which this PC is targeted to the epidermis (K5-PACE4) may be more susceptible to B(a)P complete carcinogenesis than wild type (WT) mice. In an *in vitro* experiment, using cell lines derived from skin tumors obtained after B(a)P treatment, we observed that PACE4 overexpression and activity accounts for an increased proliferation rate, exaggerated sensitivity to the PC inhibitor CMK, and interference with IGF-1R autophosphorylation. Squamous cell carcinomas, obtained from K5-PACE4 mice subjected to complete chemical carcinogenesis, were characterized by a 50 % increase in cell proliferation, when compared with similar tumors from WT mice. In addition, tumors from K5-PACE4 mice showed deeper invasion into the underlying dermis. Thus, mice overexpressing PACE4 exhibited tumors of increased growth rate and invasive potential when exposed to the human carcinogen B(a)P, further supporting the significance of PCs in tumor growth and progression.

Keywords

skin carcinogenesis; squamous cell carcinoma; benzo(a)pyrene; proprotein convertases; PACE4; PCSK6; tumor progression

INTRODUCTION

Numerous biologically active proteins require prior activation of their respective inactive protein precursors by proteolytic cleavage of an inhibiting prosegment. Subtilisine and/or kexin-related enzymes known as pro-protein convertases (PCs) achieve this activation through limited proteolysis (1-4), at the consensus motif RXX/RR[↓] (5). To date, nine mammalian Ca²⁺-dependent proteinases have been identified, including furin, PC1/PC3,

PC2, PC4, PACE4/PCSK6, PC5/PC6, PC7/LPC/PC8, SKI/S1P, and PCSK9 (3, 6-8). PACE4 (PCSK6), a well-characterized PC widely distributed in mammalian tissues, activates several biologically relevant substrates; some of them have been shown to play significant roles in tissue homeostasis and cancer growth (9-11). Among these are numerous metalloproteinases, growth factors, growth factor receptors, and adhesion molecules such as MT1-MMP, MT2-MMP TGF- β , IGF-1R, and VEGF-C are directly associated with tumor development by either modulating the degradation of the extracellular matrix (ECM), or by influencing cell adhesion and/or locomotion, as well as angiogenesis and growth (12-15).

PACE4, is expressed at low levels in many mammalian tissues and has been demonstrated to be up-regulated in various tumor cell lines and in several malignant tumors, including murine squamous cell carcinomas (SCC) induced by protocols of chemical carcinogenesis (16). In addition using transgenic mice that were designed to target PACE4 to the epidermal basal keratinocytes (K5-PACE4) we have demonstrated that this PC increased the susceptibility to skin cancer induction by a two stage chemical carcinogenesis and by UV irradiation.(17, 18)

Skin carcinogenesis models using chemical carcinogens have been used for more than a century as experimental models to understand cancer biology (19, 20). The most frequently used chemically-induced skin cancer protocol is the so-called “two stage carcinogenesis model,” which has been extremely useful to dissect the processes of tumor initiation, promotion, conversion, and progression (20, 21). Nevertheless, this protocol has been criticized for using as initiator the carcinogen 7,12-Dimethylbenz(a)anthracene (DMBA) and as promoter the phorbol ester 12-*O*-Tetradecanoylphorbol-13-acetate (TPA), both paradigmatic compounds not present in the human environment. More relevant to the development of human SCC is the ubiquitous human carcinogen benzo[a]pyrene (B(a)P), an environmental carcinogen, which plays a crucial role in the development of human tobacco-related cancers (22-24) This polycyclic aromatic hydrocarbon is a potent epithelial carcinogen that has both tumor-initiating (25-28) and tumor-promoting effects and is a potent epithelial carcinogen (29-38). This is especially true in skin, where after repetitive applications of a weekly topical dose of B(a)P (known as complete carcinogenesis) numerous primary skin tumors are induced, (31, 32, 34, 39). In addition, this protocol results in more aggressive and metastatizing cutaneous tumors than the classical two stage carcinogenesis protocol (32). Interestingly, the complete carcinogenesis protocol has been used in combination with the oncogenic virus HPV-16 in oral carcinogenesis (30) and in respiratory carcinogenesis models (40, 41), pointing to its relevance to human cancers.

Since PACE4 is involved in the processing/maturation of numerous substrates relevant to tumor invasion and metastasis (4, 16, 42), we investigated whether K5-PACE4 transgenic mice exhibit enhanced susceptibility to complete carcinogenesis, using B(a)P, than wild type mice.

MATERIALS & METHODS

Cell Lines and Transfection Procedures

We used the mouse skin cell line, derived from mouse SCC obtained by 2 stage carcinogenesis, CH72T3, (generously provided by Dr S. Fischer and C. Conti, M. D. Anderson Cancer Center Science Park, Smithville, TX) as positive control for high expression of endogenous PACE4, as well as CC4A and CC4B isolated in our laboratory as described in a previous publication (16). We included these two isogenic cell lines, derived from a low-grade SCC (CC4B) and spindle cell carcinoma (CC4A) respectively isolated from one tumor induced in SenCar mice after treatment with a complete carcinogenesis protocol with B(a)P (42, 43). All cells were grown in Spinner minimal essential medium eagle (s-MEM) medium containing 10% fetal bovine serum, 2 mM l-glutamine, and penicillin-streptomycin (Pen-Strep, Cellgro, Manassas, VA) (100 U/ml and 100 mg/ml, respectively).

Protein Convertase Enzymatic Assay

Pro-protein convertases, including PACE4, catalyze the hydrolysis of the synthetic substrate Boc-RXKR-AMC into Boc-RXKR and aminomethylcoumarine (AMC). The latter is a fluorescent compound that can be used to monitor the extent of PC activity. Reactions were performed as previously described (5, 44). Briefly, conditioned medium from cell cultures was incubated for 17 hours at 30°C in the presence of Boc-RXKR-AMC (50 µM), 100 mM HEPES (pH 7.5), 0.5% Triton X-100, and 1 mM CaCl₂. To assess the extent of CMK inhibition, we evaluated PACE4 activity in the presence of CMK (0.1-200 µM). After completion of the reaction, we measured levels of fluorescent liberated AMC using a plate reader spectrofluorometer, analyzed with the program Cary Eclipse, Varian Inc (λabsorption = 380 nm, λemission = 460 nm, 800 V of sensitivity). Experiments were repeated and performed in triplicates.

Western Blot Analyses

Protein resolution was accomplished by SDS-PAGE and Western Blot immunoblotting using 50 µg cell lysates per experimental condition as described previously (44, 45). Antibodies used for immunoblot analysis included anti-IGF-1R β-subunit (Santa Cruz Biotechnology, Inc, Santa Cruz, CA) and a monoclonal antibody anti-phospho-IGF-1R, (Cell Signaling Inc, Beverly, MA). Filters were incubated with the appropriate secondary horseradish peroxidase-conjugated antirabbit or antimouse (Amersham, Piscataway, NJ) antibodies. The processing of IGF-1R in keratinocytes was performed by culturing cell lines to 80-90% confluency, and subsequently treating cells with furin convertase inhibitor, CMK (Val-Lys-Arg-chloromethylketone, ALX-260-022, Enzo Life Sciences, Plymouth Meeting, PA) at different concentrations. Twenty-four hours after CMK treatment, the keratinocytes were lysed and subjected to Western blot analysis with polyclonal antibody against IGF-1Rβ (C-20, sc-713, Santa Cruz, CA).

Proliferation Assay

In vitro cell proliferation was measured as incorporation of [³H] methyl thymidine into DNA as described elsewhere (46, 47))

In vivo tumor induction

Tumors were induced by complete carcinogenesis protocol as previously described (29, 32, 34, 43). Briefly, eighteen wild type (WT) FVB and twenty five K5-PACE4 mice (17) were shaved and treated topically with 0.2 μmoles 3,4-Benzo[a] Pyrene (Sigma, St. Louis, MO), once a week during 40 weeks. The carcinoma volume was measured weekly and calculated using the formula: $V = [(L1 + L2)/2] \times L1 \times L2 \times 0.526$, where L1 and L2 are the length and width of the tumors. After paraffin embedding, all tumors were sectioned, stained with Hematoxylin and eosin and examined by a pathologist (AKS). Lymph nodes and lungs were also examined in the same way for the presence of metastases.

Analysis of cell proliferation in vivo

Tumor tissues were fixed in formalin, embedded in paraffin, sectioned at 4 μm, stained with H&E and Ki67 antibody using a rat monoclonal antibody (clone TEC-3, Dako, Carpinteria, CA) and a biotinylated goat anti-Rat IgG antibody (mouse pre-adsorbed) together with an ABC detection kit (Vector Elite, Vector, Burlingame, CA). Tumor cell proliferation (presented as the labeling index, LI) was determined as follows: a minimum of 500 cells per tumor (5-8 tumors per group) were counted, and the labeling index expressed as percentage of positive nuclei was calculated (18).

Immunofluorescence

Frozen sections (5 μm) from tumors were fixed in acetone, and incubated with an anti-mouse anti-collagen IV antibody (AB756P, Chemicon, Temecula, CA) for 1 hour at RT, and then treated with a FITC-labeled anti-goat IgG antibody (Jackson labs, West Grove, PA) as secondary antibody. Sections were mounted using Polong-Gold anti-fade reagent (Invitrogen, Eugene, OR). Pictures, representing a stack of Z planes, were processed using Metamorph software (Molecular Devices, Downingtown, PA). Briefly, images were 2-D deconvolved and maximum 3-D reconstructed. Nuclei were detected using the blue fluorescent dye Hoechst 33342 (17).

RESULTS

PC activity in SCC cells derived from mice treated with B(a)P

The first indication of PACE4 association with skin cancer aggressiveness arose from the isolation of two skin SCC cell lines derived from mice exposed to B(a)P (16, 32). This original study stimulated several *in vitro* and *in vivo* investigations that demonstrated increased expression of PACE4 in SCC murine cell lines, enhanced susceptibility of PACE-4 expressing K5-PACE4 transgenic mice to two stage chemical carcinogenesis and inhibition of tumor development in CMK-treated transgenic animals (16, 17, 42). Susceptibility to these inhibitory strategies depended on the levels of PACE4 expressed in the basal epidermal cells. Whereas, wild type (WT) animals showed a limited response to

the PC-inhibitor CMK, K5-PACE4 transgenic mice exhibited a marked response to this agent (42) (34).

In order to understand the contribution of PACE4 to skin tumor progression, we first studied the PC activity in cell lines derived from B(a)P treated mice, i.e., CC4A obtained from an aggressive high grade spindle cell carcinoma and CC4B, a more differentiated an less aggressive cell line derived from an isogenic SCC (16, 32)

CC4A cells expressed higher levels of PACE4 than CC4B cells (16). The differential expression of PACE4 in these two cell lines was reflected in the levels of PC-like activity; CC4A showed an enzymatic activity about 3-fold higher than that of CC4B (Figure 1 A). Furthermore, transfection of CC4B cells with the full-length PACE4 cDNA resulted in a 5-fold rise in PC proteolytic activity. This increase in enzymatic activity was blocked more than 50 % with 25 μ M CMK. Cell lines that presented high levels of PACE4 activity also showed a dramatic level of sensitivity to CMK treatment.

Both CC4A and the trasfected cell line CC4B PACE4 required only 25 μ M CMK to decrease proliferation more than 50% (Figure 1A). On the other hand, CC4B, a cell line that showed minimal PACE4 expression, did not show any significant decreased in cell proliferation at that concentration. (Figure 1B). Higher concentration of CMK resulted in a 90 % decrease in cell proliferation. Interestingly, 100 μ M CMK reduced only 50% the PC-like activity in CC4B cells transfected with PACE4. However, this concentration of CMK was capable of nearly abolishing proliferation. The exaggerated decrease in cell proliferation may be attributable in part to toxic effects of CMK. In addition, other non-PC enzymes, weakly inhibited by CMK, may play a role in this inhibition of proliferation at the highest concentrations of CMK.

Inhibition of PC activity results in marked decrease in IGF-1R processing in SCC cells

Several molecular players associated with cell proliferation contain the consensus sequence for PC's. Hence, PC-dependent activation of these proteins may be a necessary step for the increased levels of proliferation observed in many cancers. IGF-1R, mediates the insulin-like growth factors pro-proliferative responses and increases its expression in many cancers. Western blot analysis of CC4A and CC4B cell lines demonstrated that both cell lines abundantly expressed this receptor (figure 2 A), making IGF-1R suitable for the analysis of the effects of PACE4 expression on the IGF-1R-mediated cell proliferation pathway.

Despite the relatively low levels of inhibition of IGF-1R processing observed, both CC4B and CC4A cell lines failed to show IGF-1R phosphorylation/activation when stimulated by IGF-1, its natural substrate. Cells untreated with CMK were efficiently phosphorylated, even without the addition of exogenous IGF-1, probably induced by traces of endogenous IGF-1 present in the cells before induction. Pre-treatment with 10 μ M CMK resulted in the complete absence of IGF-1R phosphorylation, despite modest levels of inhibition of its processing (Figure 2 B) CC4A cells exhibited a more pronounced effect than CC4B, pointing to a stricter dependence on PACE4 activity to achieve complete IGF-1R processing and phosphorylation.

***In vivo* overexpression of PACE4 results in increased tumor cell proliferation**

The results from the previous sections could indicate that cells expressing high levels of PACE4 may have specialized in exploiting the IGF-1R pathway to drive efficient proliferation. In order to determine whether the epidermal overexpression of PACE4 will enhance the growth and aggressiveness of squamous tumors produced by complete carcinogenesis, we treated wild type and K5-PACE4 transgenic animals with weekly applications of B[a]P.

Tumor incidence was not different in wild type and transgenic mice; (Figure 3A). and the final incidence in both groups remained indistinguishable. Similarly, tumor multiplicity was not different (data not shown). Nevertheless, tumor volumes measured in K5-PACE4 mice were significantly higher ($P < 0.01$) than in WT mouse skin tumors. Moreover, the growth curves of tumors from transgenic mice fit a logarithmic pattern, indicating an initial rapid growth (approximately up to 30 weeks) that slows down during the later time points (between 30 and 41 wks) (Figure 3B). This decrease in the rate of growth may be attributed to the high density and large volume of the tumors during the late phase of carcinogenesis. On the other hand, wild type tumors showed a slow initial growth with increasingly higher rates, resembling an exponential growth.

Tumors were harvested after 41 weeks of B(a)P treatment. Skin tumor counts in transgenic mice did not significantly differ from the wild type (data not shown). Both groups of tumors exhibited similar SCC histotypes, mostly of grades I to III, i.e, well, moderately and poorly differentiated (Figure 4 A, B). Although transgenic mice had more SCCIs and SSCIIIs than the WT mice, this was not statistically significant.

Using the proliferation marker Ki-67, SCCs from transgenic mice exhibit higher number of positively stained tumor cells than SCCs from WT mice (Figure 4 C and D). This increase was of approximately 50%; labeling index of transgenic K5-PACE4 tumors was 47%, whereas that of WT tumors was 29%; (Figure 4E) ($P < 0.001$). These results point to a predominant PACE4 pro-proliferative effect.

Overexpression of PACE4 results in increased depth of invasion, degradation of collagen IV, and lung metastasis

In order to determine if ectopic expression of PACE4 in SCCs from transgenic mice differed in their *in vivo* invasive ability from those that grew in WT mice, we measured the penetration of cancer cells into the underlying dermis and subcutaneous tissue (Figure 5 A-D). This showed a significant tendency ($P < 0.002$) for deeper penetration of tumor cells in K5-PACE4 mice with respect to WT mice (2.7 mm penetration in K5-PACE4 mice versus 2.1 mm penetration in WT mice (Figure 5 E).

The increased penetration into the underlying sub-epidermal tissues correlated with the known alteration of the basement membrane (bm) of the epidermal basal layer (17). Most tumors from the K5-PACE4 mice showed a thinner or absent bm as revealed by immunofluorescence of tumor sections stained with anti-collagen IV antibody. This contrasted with the thicker and more robustly delineated bm in SCCs from WT mice (Figure 5 F and G).

DISCUSSION

Previous publications from our laboratory demonstrated that most mouse SCC cell lines expressed higher levels of PACE4 (including messenger RNA, protein, and enhanced proteolytic activity) than cell lines derived from normal murine keratinocytes or from either papillomas or low grade SCCs (44, 48). Other PCs, such as Furin and PC5, did not show this clear tendency in murine cell lines (44). Furin was expressed at moderate levels in nearly all cell lines, whereas PC5 was not detected. PC7 expression increased moderately from normal to cancer cell lines. Interestingly the cell lines with the highest PACE4 expression exhibited the highest PC activity (CC4A and CH72T3) (16, 44).

Herein we report the screening of several cell lines derived from murine tumors, including the isogenic CC4A, CC4B cells and CC4B cells transfected with the full-length PACE4 cDNA for PC-like activity. Mirroring the levels of expression previously reported (16, 44, 48), both parental and mock-transfected CC4B showed very low levels of PC activity. In contrast, CC4A and PACE-4-transfected CC4B showed the highest PC activity levels. Previously we reported that these cell lines did not significantly differ in the expression of the other ubiquitous PCs, such as furin, PC5 or PC7 (44), suggesting that these differences in activity may be attributed to PACE4.

To study the effects of increased expression of PACE4 on cell lines, we blocked PC's activity with the PC inhibitor CMK (49), and analyzed the processing of one of the most important PC substrate associated with proliferation and survival; IGF-1R. CMK decreased the processing of this receptor in modest amounts; however, it completely abolished its IGF-1-induced autophosphorylation. This lack of phosphorylation suggests a complete blockage of the downstream signaling that leads to increased proliferation, decreased apoptosis and enhanced survival.

As a receptor tyrosine kinase, IGF-1R undergoes dimerization and phosphorylation. A truncated form lacking the C-terminal domain that lacks the phosphorylation domain while retaining the ligand binding site exerts a dominant negative effect (50). Likewise, overexpression of an IGF-1R mutant unable to bind ATP in the cytoplasmic domain behaves as a dominant negative, precluding receptor phosphorylation (51). One interesting clinical case describes a decreased ligand binding, receptor phosphorylation, cell proliferation and body growth in a child carrying a furin cleavage site mutation, preventing furin processing (52). These studies support the idea that the presence of unprocessed IGF-1R interferes with the wild type receptor phosphorylation, probably by decreasing dimerization, phosphorylation or both, explaining the lack of phosphorylation in CMK-treated cells.

Proliferation assays that measure DNA synthesis showed that CMK sensitivity was dependent on both PACE4 expression and PC-activity. CC4A, the cell line that expressed high levels of endogenous PACE4, proved to have an increased sensitivity to CMK indicating that elevated expression of PACE4 may also promote the dependence of this PC to proliferate, making it a potential target to decrease tumor cell proliferation in those cells that exhibit high expression of PACE4. In contrast, CC4B, characterized by lower PACE4 expression, proved to be less sensitive to CMK, requiring higher concentrations to achieve a

measurable inhibitory effect on cell proliferation, suggesting that this cell line relies more on other alternative, PC-independent mechanisms to drive proliferation. Strikingly, CC4B cells transfected with the full-length PACE4 cDNA showed a drastic increase in CMK sensitivity, noticed as a 70% decrease in proliferation, supporting a role of PACE4 in CMK sensitivity and a switch to PC-dependent proliferative pathways. This dependence on PC-associated pathways, including IGF-1R, may result in increased proliferation, survival, and invasive potential in tumors expressing PACE4. CC4A cells were more sensitive to CMK in terms of blockage of IGF-1R processing. After CMK treatment, the proform, pro-IGF-1R represents a 17% and 10% of the mature form in CC4A and CC4B, respectively. This result points to a modest, but greater effect of CMK on CC4A cells than on CC4B cells.

Next, we sought to extend these observations to animals, using a physiologically relevant *in vivo* carcinogenesis model. In previous experiments, we showed that K5-PACE4 transgenic mice expressing the complete coding sequence for PACE4 targeted to the basal layer of the epidermis developed twice as many carcinomas that wild type mice using a two-stage carcinogenesis protocol (17). In addition, PACE4 transgenic animals exhibited increased ability to activate MT1-MMP and MT2-MMP resulting in early degradation of the collagen IV component of the basement membrane (17) in a way that closely resembles the effect of the complete carcinogenesis protocol used in the present report.

The complete carcinogenesis protocol with B(a)P has been used to study skin carcinogenesis because of the easy accessibility to the cutaneous surface and similarities with head and neck epithelia. Because of the continuous mutagenic and promoting activity results in higher incidence of primary SCC and metastases this model is a better approximation to human SCCs of several sites than the two stage carcinogenesis skin model (32-33). Thus, mouse skin/epidermal carcinogenesis has been used as a model for tobacco-associated squamous cell carcinoma (39). The obvious differences notwithstanding, it is an acceptable system to study the etiopathogenesis, biology, and prevention of lung and upper aero-digestive tract cancer (34, 39).

Because PACE4 overexpression also increases tumor susceptibility, this experiment was planned to evaluate if K5-PACE4 mice would be susceptible to the human carcinogen B(a)P and whether this treatment would result in SCCs of advanced malignant phenotype. Surprisingly, in these experiments there was no significant difference between transgenic and WT mice with respect to SCC incidence, multiplicity and histotype. Nevertheless, we found that tumor volume and growth were significantly higher in transgenic mice than in WT mice. Tumor growth in transgenic mice was seen relatively early and this resulted in rapid growth in volume and a persistent higher Ki-67 labeling index than in WT SCCs. The fast initial growth rate was reflected in higher tumor incidence in the transgenic mice in earlier time points during carcinogenesis. At later time points, growth rate decreases and a similar incidence and tumor multiplicity were observed in both groups, while tumor size remains much higher in K5-PACE4 mice ($P < 0.01$). This was also accompanied by a much higher labeling index of SCC in K5-PACE4 mice than in WT mice ($P < 0.001$). The increase in volume and Ki-67 labeling index in transgenics is the consequence of the well-known processing of growth factors and their receptors that characterize pro-protein convertases such as PACE4 (4,23). Interestingly, *in vivo* growth of knocked down human prostate cancer

cells showed complementary results (53). The comparison between the two very different models reveals that PACE4 has a very effective role in controlling tumor cell proliferation *in vivo*. Whereas, Couture et al (53) describe an approximately 50% decrease of cell proliferation in human xenotransplanted PACE4 knockdown prostate cancer cells, in our model of murine PACE4 transgenic skin tumors we demonstrated a similar increase in proliferation in SCCs from K5-PACE4 mice when compared to WT tumors. In addition, in the prostate cell xenotransplantation model, PACE4 was the main factor in proliferation regulation when compared to PC7 and furin that had little or no effect on tumor cell proliferation.

In addition to PACE4's pro-proliferative effect, the processing of invasion associated-PC substrates such as MMPs (4, 9, 23) are the probable cause of the increased dermal invasiveness observed in K5-PACE4 mice.

Taken together, this data on K5-PACE4 mice shows that complete skin carcinogenesis with the human carcinogen B(a)P results in tumors of increased growth rates and invasive potential in mice overexpressing the proprotein convertase.

This data permits to speculate that, perhaps in the near future, patients presenting high tumor levels of PC will become candidates for PC-inhibiting treatment approaches that could diminish the invasive ability of cancer cells.

ACKNOWLEDGEMENTS

We thank the following core facilities at Fox Chase Cancer Center for their help: Histopathology Facility, Transgenic Mouse Facility, Laboratory Animal Facility, and the Biostatistics and Bioinformatics Facility. This work was supported by grants from the National Institutes of Health, R01-CA133001 (AKS), R01-CA75028 (AKS) R01-CA113451 (EC) and, P30-CA06927, as well as by an appropriation from the Commonwealth of Pennsylvania and a grant from American Cancer Research Center and Foundation. The content is solely the responsibility of the authors and does not necessarily represent the official views of the National Cancer Institute or the National Institutes of Health and the other funding agencies.

List of Abbreviations

| | |
|--------------|--------------------------------|
| AMC | aminomethylcoumarine |
| B(a)P | 3,4-benzo(a)pyrene |
| CMK | Val-Lys-Arg-chloromethylketone |
| PC | proprotein convertases |
| SCC | squamous cell carcinoma |
| WT | Wild type |

REFERENCES

1. Steiner DF. The proprotein convertases. *Curr Opin Chem Biol.* 1998; 2:31–9. [PubMed: 9667917]
2. Seidah NG, Day R, Marcinkiewicz M, Chretien M. Precursor convertases: an evolutionary ancient, cell-specific, combinatorial mechanism yielding diverse bioactive peptides and proteins. *Ann N Y Acad Sci.* 1998; 839:9–24. [PubMed: 9629127]

3. Seidah NG, Chretien M. Proprotein and prohormone convertases: a family of subtilases generating diverse bioactive polypeptides. *Brain Res.* 1999; 848:45–62. [PubMed: 10701998]
4. Bassi DE, Mahloogi H, Klein-Szanto AJ. The proprotein convertases furin and PACE4 play a significant role in tumor progression. *Mol Carcinog.* 2000; 28:63–9. [PubMed: 10900462]
5. Molloy SS, Bresnahan PA, Leppla SH, Klimpel KR, Thomas G. Human furin is a calcium-dependent serine endoprotease that recognizes the sequence Arg-X-X-Arg and efficiently cleaves anthrax toxin protective antigen. *J Biol Chem.* 1992; 267:16396–402. [PubMed: 1644824]
6. Seidah NG, Benjannet S, Wickham L, Marcinkiewicz J, Jasmin SB, Stifani S, et al. The secretory proprotein convertase neural apoptosis-regulated convertase 1 (NARC-1): Liver regeneration and neuronal differentiation. *P Natl Acad Sci USA.* 2003; 100:928–33.
7. Seidah NG, Chretien M. Eukaryotic protein processing: endoproteolysis of precursor proteins. *Curr Opin Biotechnol.* 1997; 8:602–7. [PubMed: 9353231]
8. Toure BB, Munzer JS, Basak A, Benjannet S, Rochemont J, Lazure C, et al. Biosynthesis and enzymatic characterization of human SKI-1/S1P and the processing of its inhibitory prosegment. *J Biol Chem.* 2000; 275:2349–58. [PubMed: 10644685]
9. Tsuji A, Sakurai K, Kiyokage E, Yamazaki T, Koide S, Toida K, et al. Secretory proprotein convertases PACE4 and PC6A are heparin-binding proteins which are localized in the extracellular matrix. Potential role of PACE4 in the activation of proproteins in the extracellular matrix. *Biochim Biophys Acta.* 2003; 1645:95–104. [PubMed: 12535616]
10. Tsuji A, Hashimoto E, Ikoma T, Taniguchi T, Mori K, Nagahama M, et al. Inactivation of proprotein convertase, PACE4, by alpha1-antitrypsin Portland (alpha1-PDX), a blocker of proteolytic activation of bone morphogenetic protein during embryogenesis: evidence that PACE4 is able to form an SDS-stable acyl intermediate with alpha1-PDX. *J Biochem.* 1999; 126:591–603. [PubMed: 10467177]
11. Yuasa K, Masuda T, Yoshikawa C, Nagahama M, Matsuda Y, Tsuji A. Subtilisin-like proprotein convertase PACE4 is required for skeletal muscle differentiation. *J Biochem.* 2009; 146:407–15. [PubMed: 19520771]
12. Dubois CM, Blanchette F, Laprise MH, Leduc R, Grondin F, Seidah NG. Evidence that furin is an authentic transforming growth factor-beta1-converting enzyme. *Am J Pathol.* 2001; 158:305–16. [PubMed: 11141505]
13. Yana I, Weiss SJ. Regulation of membrane type-1 matrix metalloproteinase activation by proprotein convertases. *Mol Biol Cell.* 2000; 11:2387–401. [PubMed: 10888676]
14. Sato H, Kinoshita T, Takino T, Nakayama K, Seiki M. Activation of a recombinant membrane type 1-matrix metalloproteinase (MT1-MMP) by furin and its interaction with tissue inhibitor of metalloproteinases (TIMP)-2. *FEBS Lett.* 1996; 393:101–4. [PubMed: 8804434]
15. Khatib AM, Siegfried G, Prat A, Luis J, Chretien M, Metrakos P, et al. Inhibition of proprotein convertases is associated with loss of growth and tumorigenicity of HT-29 human colon carcinoma cells: importance of insulin-like growth factor-1 (IGF-1) receptor processing in IGF-1-mediated functions. *J Biol Chem.* 2001; 276:30686–93. [PubMed: 11402025]
16. Hubbard FC, Goodrow TL, Liu SC, Brilliant MH, Basset P, Mains RE, et al. Expression of PACE4 in chemically induced carcinomas is associated with spindle cell tumor conversion and increased invasive ability. *Cancer Res.* 1997; 57:5226–31. [PubMed: 9393739]
17. Bassi DE, Lopez De Cicco R, Cenna J, Litwin S, Cukierman E, Klein-Szanto AJ. PACE4 expression in mouse basal keratinocytes results in basement membrane disruption and acceleration of tumor progression. *Cancer Res.* 2005; 65:7310–9. [PubMed: 16103082]
18. Fu J, Bassi DE, Zhang J, Li T, Cai KQ, Testa CL, et al. Enhanced UV-induced skin carcinogenesis in transgenic mice overexpressing proprotein convertases. *Neoplasia.* 2013; 15(2):169–79. PMID: 3579319. [PubMed: 23441131]
19. Shimkin MB, Triolo VA. History of chemical carcinogenesis: some prospective remarks. *Prog Exp Tumor Res.* 1969; 11:1–20. [PubMed: 4890070]
20. DiGiovanni J. Multistage carcinogenesis in mouse skin. *Pharmacol Ther.* 1992; 54:63–128. [PubMed: 1528955]
21. Slaga TJ. Overview of tumor promotion in animals. *Environ Health Perspect.* 1983; 50:3–14. [PubMed: 6347683]

22. Hecht SS. Cigarette smoking and lung cancer: chemical mechanisms and approaches to prevention. *Lancet Oncol.* 2002; 3(8):461–9. [PubMed: 12147432]
23. Denissenko MF, Pao A, Tang M, Pfeifer GP. Preferential formation of benzo[a]pyrene adducts at lung cancer mutational hotspots in P53. *Science.* 1996; 274:430–2. [PubMed: 8832894]
24. Yoshino I, Kometani T, Shoji F, Osoegawa A, Ohba T, Kouso H, et al. Induction of epithelial-mesenchymal transition-related genes by benzo[a]pyrene in lung cancer cells. *Cancer.* 2007; 110:369–74. [PubMed: 17559143]
25. Siddens LK, Larkin A, Krueger SK, Bradfield CA, Waters KM, Tilton SC, et al. Polycyclic aromatic hydrocarbons as skin carcinogens: comparison of benzo[a]pyrene, dibenzo[def,p]chrysene and three environmental mixtures in the FVB/N mouse. *Toxicol Appl Pharmacol.* 2012; 264:377–86. PMID: 3483092. [PubMed: 22935520]
26. Nesnow S, Gold A, Sangaiah R, Slaga TJ. Mouse skin tumor-initiating activity of benz[j]aceanthrylene in SENCAR mice. *Cancer Lett.* 1993; 73(2-3):73–6. [PubMed: 8221632]
27. Nesnow S, Triplett LL, Slaga TJ. Studies on the tumor initiating, tumor promoting, and tumor co-initiating properties of respiratory carcinogens. *Carcinog Compr Surv.* 1985; 8:257–77. [PubMed: 3986826]
28. Slaga TJ, Bracken WM, Dresner S, Levin W, Yagi H, Jerina DM, et al. Skin tumor-initiating activities of the twelve isomeric phenols of benzo(a)pyrene. *Cancer Res.* 1978; 38:678–81. [PubMed: 626971]
29. Slaga TJ, Fischer SM, Weeks CE, Klein-Szanto AJ. Multistage chemical carcinogenesis in mouse skin. *Curr Probl Dermatol.* 1980; 10:193–218. [PubMed: 6786833]
30. Park NH, Gajuluva CN, Baek JH, Cherrick HM, Shin KH, Min BM. Combined oral carcinogenicity of HPV-16 and benzo(a)pyrene: an in vitro multistep carcinogenesis model. *Oncogene.* 1995; 10:2145–53. [PubMed: 7784058]
31. Mitsunaga S, Clapper M, Litwin S, Watts P, Bauer B, Klein-Szanto AJ. Chemopreventive effect of difluoromethylornithine (DFMO) on mouse skin squamous cell carcinomas induced by benzo(a)pyrene. *J Cell Biochem Suppl.* 1997; 28-29:81–9. [PubMed: 9589352]
32. Ruggeri B, DiRado M, Zhang SY, Bauer B, Goodrow T, Klein-Szanto AJ. Benzo[a]pyrene-induced murine skin tumors exhibit frequent and characteristic G to T mutations in the p53 gene. *Proc Natl Acad Sci U S A.* 1993; 90:1013–7. [PubMed: 8430068]
33. Guttenplan JB, Kosinska W, Zhao ZL, Chen KM, Aliaga C, DelTondo J, et al. Mutagenesis and carcinogenesis induced by dibenzo[a,l]pyrene in the mouse oral cavity: a potential new model for oral cancer. *Int J Cancer.* 2012; 130:2783–90. [PubMed: 21815141]
34. Bassi DE, Klein-Szanto AJ. Carcinogen-induced animal models of head and neck squamous cell carcinoma. *Curr Protoc Pharmacol.* 2007 Chapter 14:Unit 14 2.
35. Zhao P, Fu J, Yao B, Song Y, Mi L, Li Z, et al. In vitro malignant transformation of human bronchial epithelial cells induced by benzo(a)pyrene. *Toxicol In Vitro.* 2012; 26:362–8. [PubMed: 22227536]
36. Iizasa T, Momiki S, Bauer B, Caamano J, Metcalf R, Lechner J, et al. Invasive tumors derived from xenotransplanted, immortalized human cells after in vivo exposure to chemical carcinogens. *Carcinogenesis.* 1993; 14:1789–94. [PubMed: 8403201]
37. Sellakumar AR, Montesano R, Saffiotti U, Kaufman DG. Hamster respiratory carcinogenesis induced by benzo(a)pyrene and different dose levels of ferric oxide. *J Natl Cancer Inst.* 1973; 50:507–10. [PubMed: 4702121]
38. Ashurst SW, Cohen GM, Nesnow S, DiGiovanni J, Slaga TJ. Formation of benzo(a)pyrene/DNA adducts and their relationship to tumor initiation in mouse epidermis. *Cancer Res.* 1983; 43:1024–9. [PubMed: 6297716]
39. Walaszek Z, Hanausek M, Slaga TJ. The role of skin painting in predicting lung cancer. *Int J Toxicol.* 2007; 26:345–51. [PubMed: 17661226]
40. Saffiotti U, Montesano R, Sellakumar AR, Cefis F, Kaufman DG. Respiratory tract carcinogenesis in hamsters induced by different numbers of administrations of benzo(a)pyrene and ferric oxide. *Cancer Res.* 1972; 32:1073–81. [PubMed: 4336025]

41. Saffiotti U, Montesano R, Sellakumar AR, Kaufman DG. Respiratory tract carcinogenesis induced in hamsters by different dose levels of benzo-(a)pyrene and ferric oxide. *J Natl Cancer Inst.* 1972; 49:1199–204. [PubMed: 5084126]
42. Mahloogi H, Bassi DE, Klein-Szanto AJ. Malignant conversion of non-tumorigenic murine skin keratinocytes overexpressing PACE4. *Carcinogenesis.* 2002; 23:565–72. [PubMed: 11960907]
43. Ruggeri BA, Bauer B, Zhang SY, Klein-Szanto AJ. Murine squamous cell carcinoma cell lines produced by a complete carcinogenesis protocol with benzo[a]pyrene exhibit characteristic p53 mutations and the absence of H-ras and cyclin D1 abnormalities. *Carcinogenesis.* 1994; 15:1613–9. [PubMed: 8055640]
44. Bassi DE, Zhang J, Cenna J, Litwin S, Cukierman E, Klein-Szanto AJ. Proprotein convertase inhibition results in decreased skin cell proliferation, tumorigenesis, and metastasis. *Neoplasia.* 2010; 12:516–26. [PubMed: 20651981]
45. Lopez de Cicco R, Watson JC, Bassi DE, Litwin S, Klein-Szanto AJ. Simultaneous expression of furin and vascular endothelial growth factor in human oral tongue squamous cell carcinoma progression. *Clin Cancer Res.* 2004; 10:4480–8. [PubMed: 15240540]
46. Khatib AM, Siegfried G, Prat A, Luis J, Chretien M, Metrakos P, et al. Inhibition of proprotein convertases is associated with loss of growth and tumorigenicity of HT-29 human colon carcinoma cells - Importance of insulin-like growth factor-1 (IGF-1) receptor processing in IGF-1-mediated functions. *Journal of Biological Chemistry.* 2001; 276:30686–93. [PubMed: 11402025]
47. Bassi DE, Mahloogi H, De Cicco RL, Klein-Szanto A. Increased furin activity enhances the malignant phenotype of human head and neck cancer cells. *American Journal of Pathology.* 2003; 162:439–47. [PubMed: 12547702]
48. Mahloogi H, Gonzalez-Guerrico AM, Lopez De Cicco R, Bassi DE, Goodrow T, Braunewell KH, et al. Overexpression of the calcium sensor visinin-like protein-1 leads to a cAMP-mediated decrease of in vivo and in vitro growth and invasiveness of squamous cell carcinoma cells. *Cancer Res.* 2003; 63:4997–5004. [PubMed: 12941826]
49. Anglikier H. Synthesis of tight binding inhibitors and their action on the proprotein-processing enzyme furin. *J Med Chem.* 1995; 38:4014–8. [PubMed: 7562936]
50. Sachdev D, Hartell JS, Lee AV, Zhang X, Yee D. A dominant negative type I insulin-like growth factor receptor inhibits metastasis of human cancer cells. *J Biol Chem.* 2004; 279:5017–24. [PubMed: 14615489]
51. Cheng ZQ, Adi S, Wu NY, Hsiao D, Woo EJ, Filvaroff EH, et al. Functional inactivation of the IGF-I receptor delays differentiation of skeletal muscle cells. *J Endocrinol.* 2000; 167:175–82. [PubMed: 11018765]
52. Kawashima Y, Kanzaki S, Yang F, Kinoshita T, Hanaki K, Nagaishi J, et al. Mutation at cleavage site of insulin-like growth factor receptor in a short-stature child born with intrauterine growth retardation. *J Clin Endocrinol Metab.* 2005; 90:4679–87. [PubMed: 15928254]
53. Couture F, D'Anjou F, Desjardins R, Boudreau F, Day R. Role of proprotein convertases in prostate cancer progression. *Neoplasia.* 2012; 14:1032–42. [PubMed: 23226097]

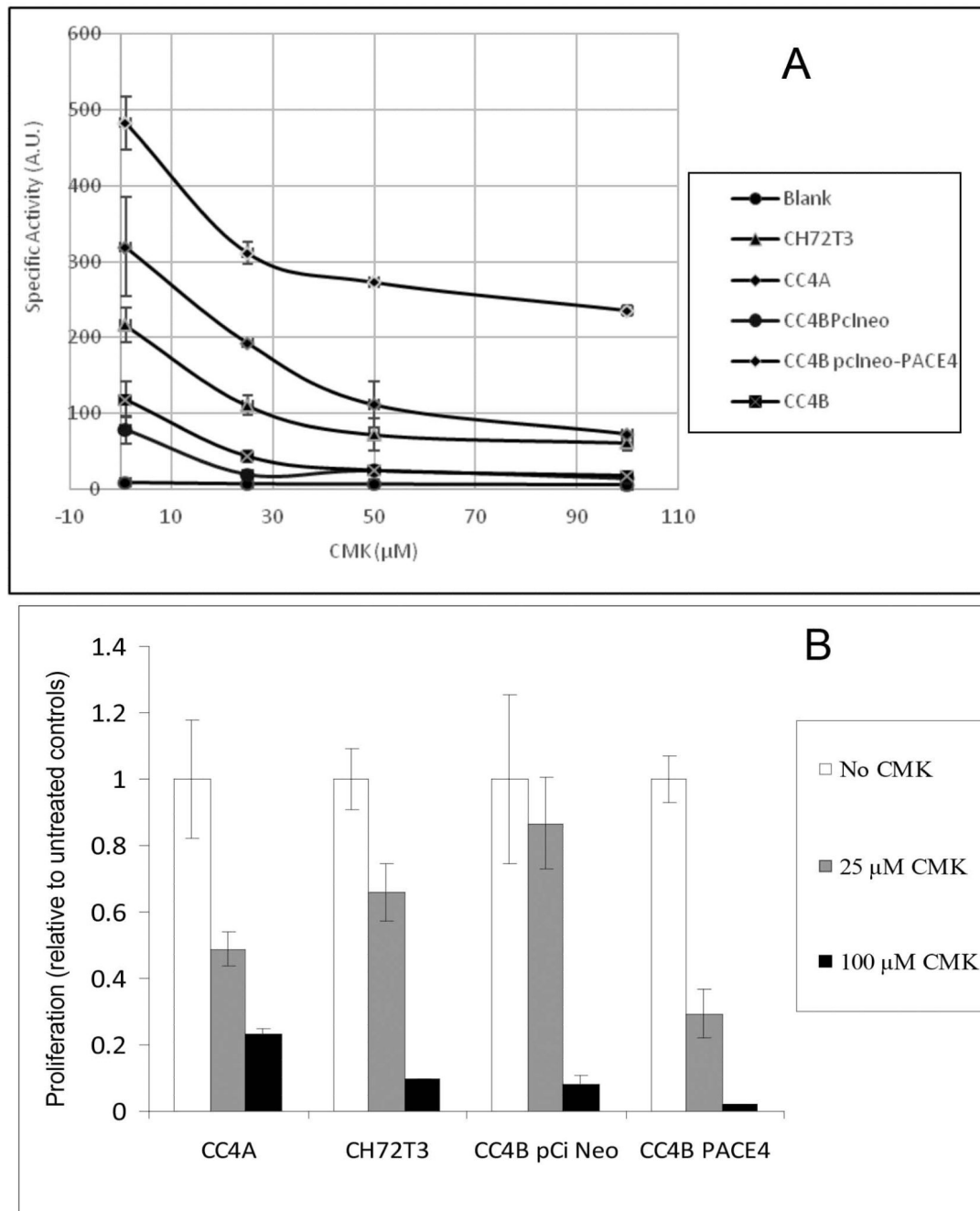


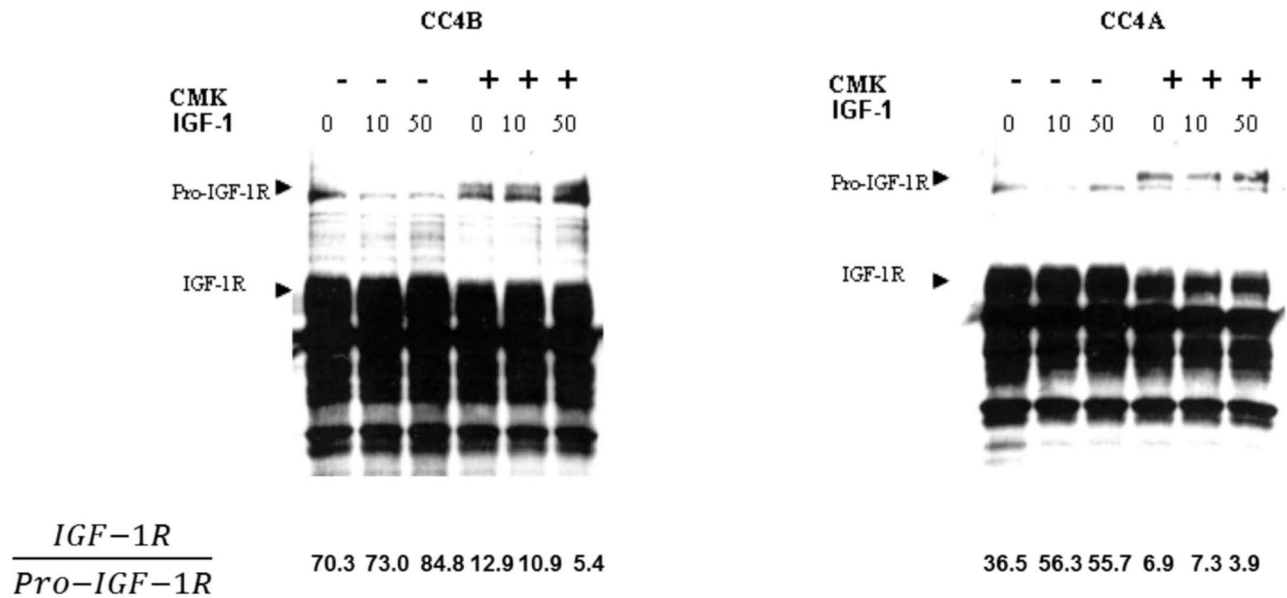
Figure 1.

A: Inhibition of PC activity using CMK. Three concentrations of CMK were added to the cell culture medium of four murine SCC cell lines. Cells were incubated overnight with serum- and phenol red-free medium. Following concentration of the conditioned medium, PC activity was determined in the presence and absence of CMK. Note that cells expressing PACE4 (CC4BpCi PACE4, CC4A and CH72T3) show marked inhibition with 25 and 50 μM , whereas CC4B pCi Neo cells and the parental cell line CC4B, that have minimal

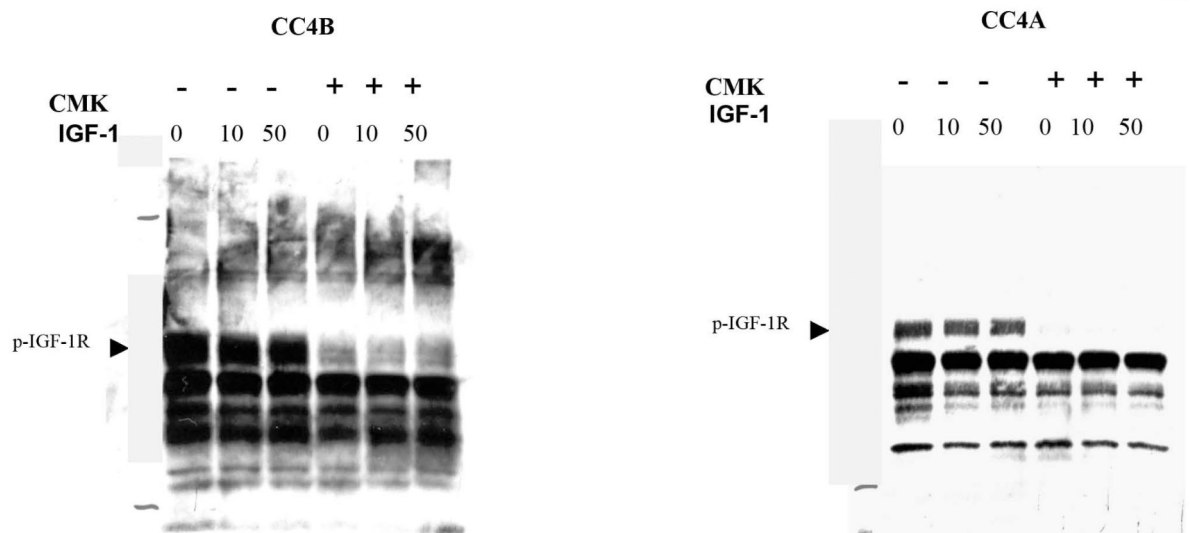
PACE4 expression, showed marginal levels of PC inhibition. CH72T3 is a SCC line overexpressing endogenous PACE4 (16) used as positive control.

B: Effect of CMK on cell proliferation rates. Proliferation rates, calculated as the ratio of newly synthesized DNA in the presence and absence of CMK. Note that cells expressing PACE4 show a more pronounced inhibition of proliferation CC4B pCi Neo cells (mocked transfected cell that have minimal PACE4 expression) when incubated in the presence of 25 μ M CMK.

A



B

**Figure 2.**

Effect of CMK on IGF-1R processing (A) and phosphorylation. (B). CC4A and CC4B cells where incubated in the presence or absence of CMK. After 48 hours, cells were washed and incubated with two different IGF-1 concentrations for 10 minutes. Proteins from the IGF-1-induced cells were extracted and analyzed using SDS-PAGE followed by immunoblotting. Note the reduction in full-processed form and the presence of the unprocessed form, detected only in CMK treatments (A). The receptor was not phosphorylated in the presence of CMK, even after induction with high concentration of IGF-1. After densitometric measurements were obtained, the ratio of processed (IGF-1R) to unprocessed (Por-IGF-1R)

were calculated and indicated at the bottom of panel A. Notice the decrease ratio of processed/unprocessed after CMK treatment.

Author Manuscript

Author Manuscript

Author Manuscript

Author Manuscript

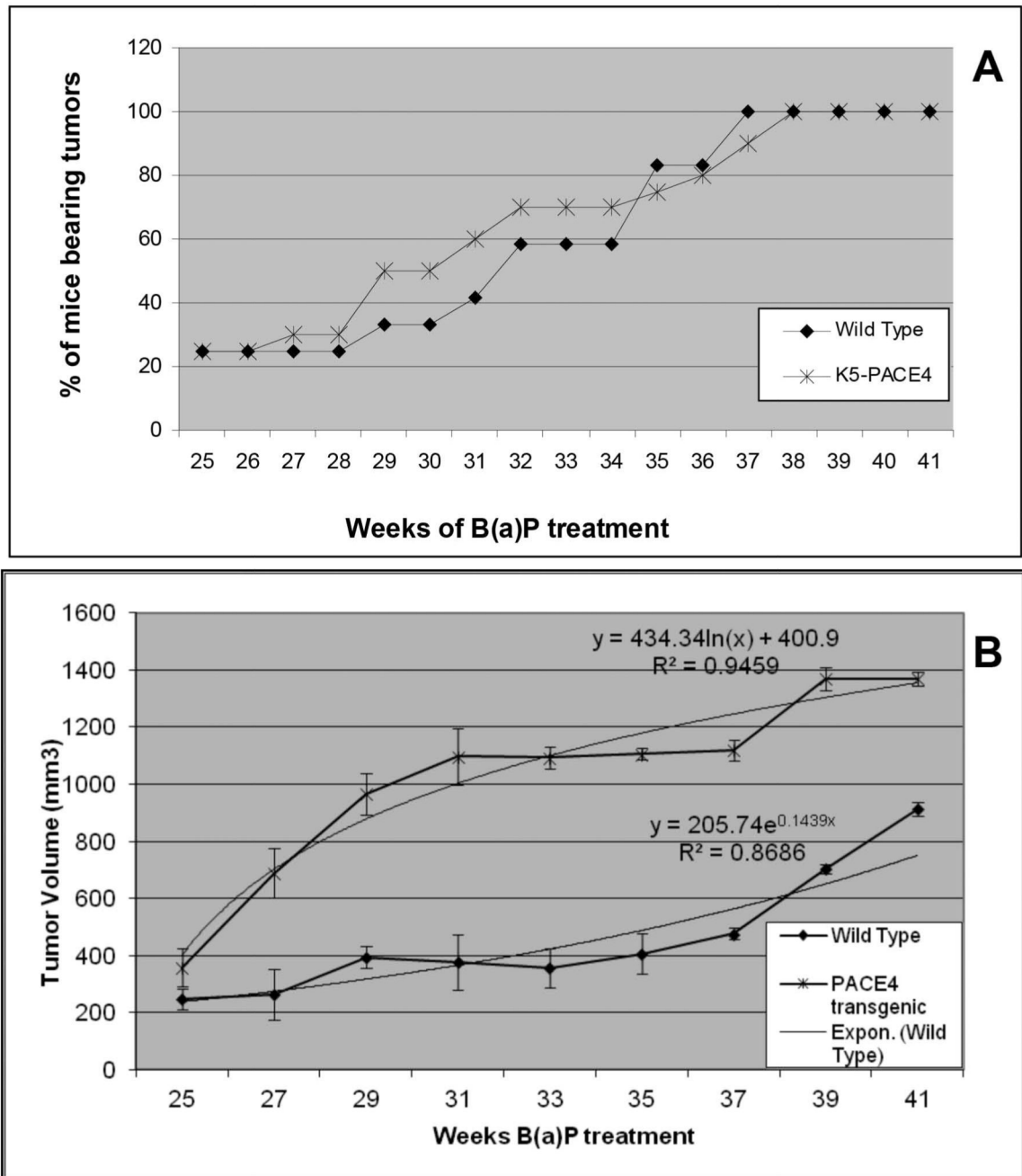


Figure 3. Tumor Multiplicity and Volume. A: Percent of animals bearing skin tumors during complete carcinogenesis. Note that there is a small window between weeks 28 and 35 weeks in which the transgenic mice show a mild increase in animals with tumors. Otherwise both WT and K5-PACE4 mice showed similar tumor incidence. B: Tumor volume was significantly higher ($P < 0.01$) in K5-PACE4 mice when compared with WT control animals. Each point represents the mean and the bars the SEM.

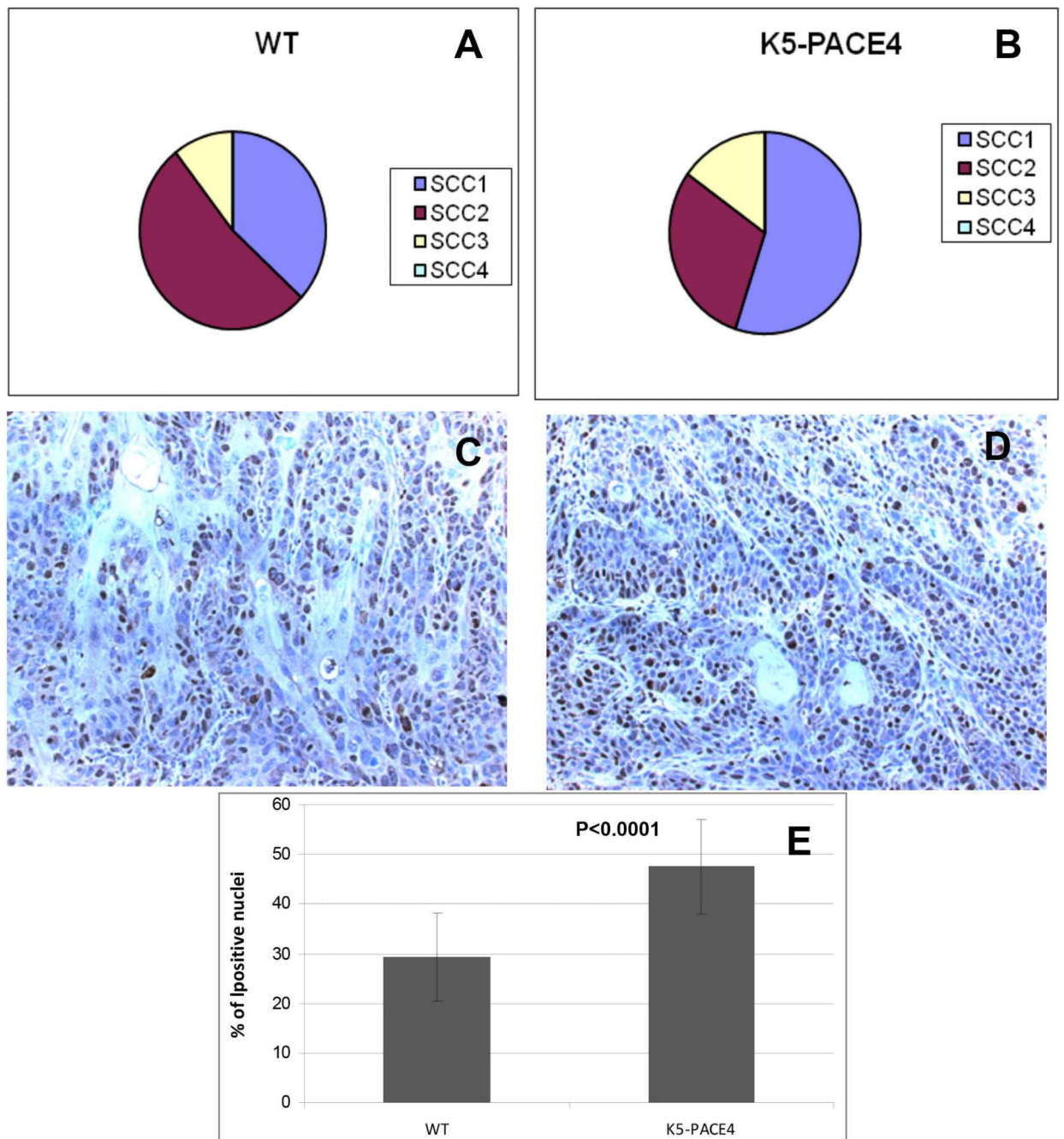


Figure 4. SCC Histotypes and proliferation rates. Pie charts show the proportion of different SCC phenotypes in WT and K5-PACE4 transgenic mice (A and B). Panel C shows a SCC from a WT mouse with numerous Ki67 labeled nuclei. Panel D: shows a similar SCC from a K5-PACE4 mouse showing even more numerous Ki67 labeled nuclei. E: Histogram showing the Ki67 labeling index (% of positively stained tumor nuclei) in WT and K5-PACE4 mice tumors. Note increase of more than 50% in K5-PACE4 mice ($p < 0.001$).

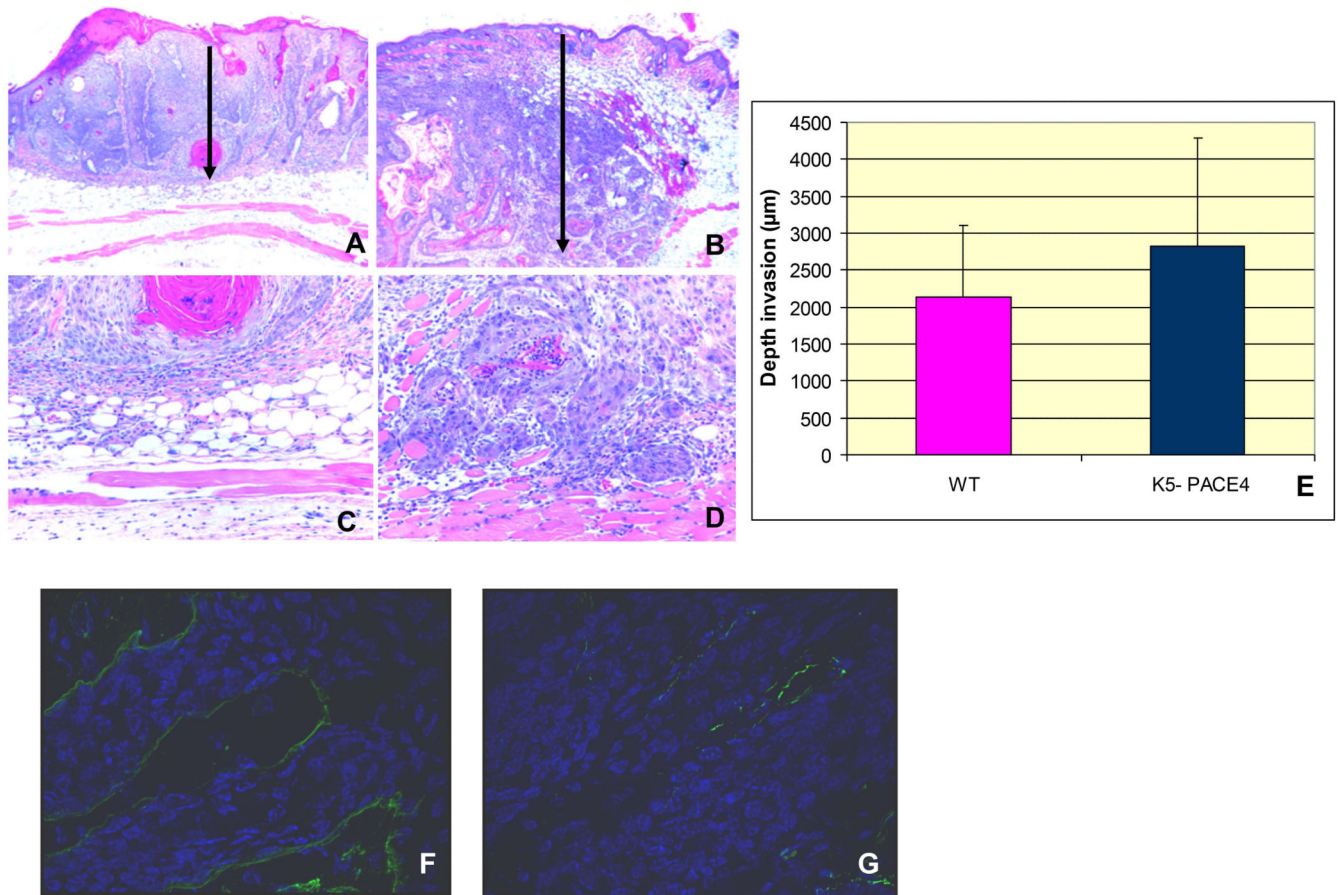


Figure 5.

PACE4-dependent enhancement of dermal invasion: Panel A shows a SCC from a WT mouse invading the superficial and deep dermis but sparing the subcutaneous and muscle layers (see panel C for larger magnification). Panel B depicts an SCC from a K5-PACE4 mouse invading the dermis as well as the subcutaneous and muscle tissues (see panel D for larger magnification). The vertical arrows in these panels depict the depth of invasion. The histogram shows the depth of penetration (expressed in micrometers) into the subepidermal tissues in both animal groups ($p < 0.002$) (E). Immunofluorescence of Collagen IV in WT (F) and K5-PACE4 animals (G). Note that the basement membrane is practically intact and quite extensive in WT mice (F), whereas in the K5-PACE4 mice (G) it is less abundant, fragmented and discontinuous.